

HTXRD Study of The Crystal Structure of SrZrO₃ Using a New Capillary Furnace for Synchrotron XRD at X14A

X14A and the HTML User Program

**Scott Speakman, Jianming Bai,
Andrew Payzant and Camden R. Hubbard**

27 January 2005

NSLS Workshop on Structure Solution



**OAK RIDGE NATIONAL LABORATORY
U.S. DEPARTMENT OF ENERGY**

Outline

- **SrZrO₃ Structure Determination above 725 °C**
- **My Group, the X14A PRT and X14A Summary**
- **Acknowledgements**
 - **High Temperature Materials Laboratory User Program**

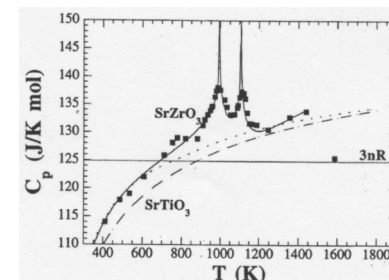
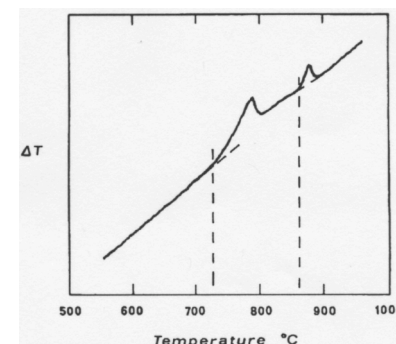
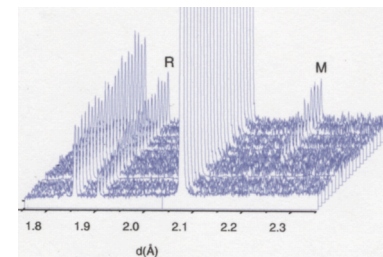


The transition path of SrZrO₃ has been extensively studied, but discrepancies still remain

S. Speakman, E.A. Payzant, & J. Bai (ORNL, UT)

- The phase transitions of SrZrO₃ have been studied by:
 - High-temperature X-ray and neutron diffraction
 - Carlsson, 1967; Ahtee et al. 1978; de Ligny and Richet, 1996; Kennedy et al., 1999; Howard et al., 2000; Payzant et al., 2000
 - Differential thermal analysis (Carlsson, 1967)
 - Drop calorimetry (de Ligny and Richet, 1996)
- There are four distinct phases:

Phase	T _C (°C) by de Ligny and Richet	Reported T _C 's (°C)
Orthorhombic Pnma		
Orthorhombic Cmcm or Metrically Tetragonal Imma	727±5	700 to 750
Tetragonal I4/mcm	832±5	747 to 860
Cubic Pm3m	1167±25	1070 to 1170



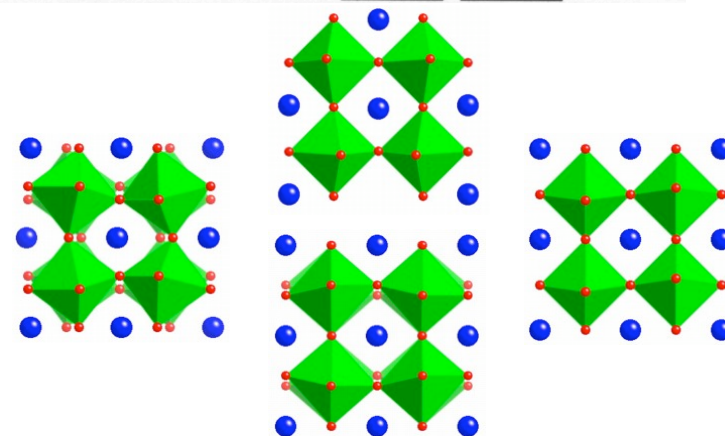
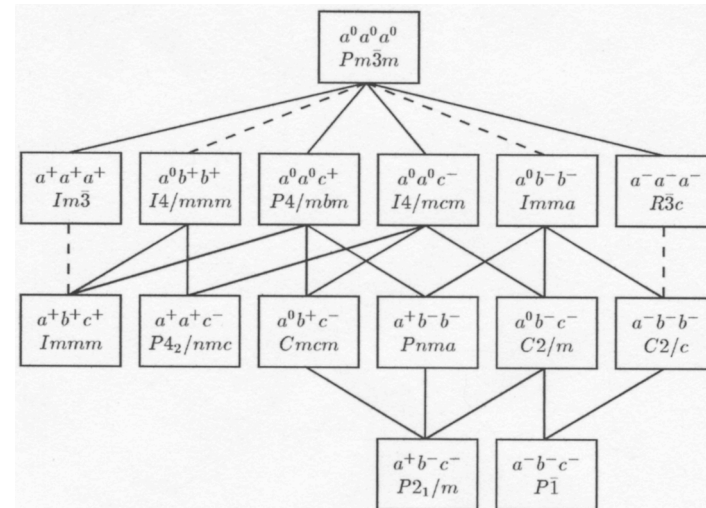
The engineering of material properties in perovskites relies on proper understanding of octahedral tilting

- Perovskites possess technologically important properties
 - pyro- and piezo-electricity
 - dielectric susceptibility
 - linear and non-linear electrooptic effects
- The tilting of anion octahedra and displacement of cations have significant effects on material properties of perovskites
 - Slight structural changes can have enormous effects
 - The loss of ferroelectric or piezoelectric behavior at the Curie temperature
 - Changes in dielectric constant by as much as a factor of 10^4
 - Changes in electronic and ionic conductivity by orders of magnitude
- Understanding of these slight variations in crystal structure are critical to understanding the behavior of perovskite materials



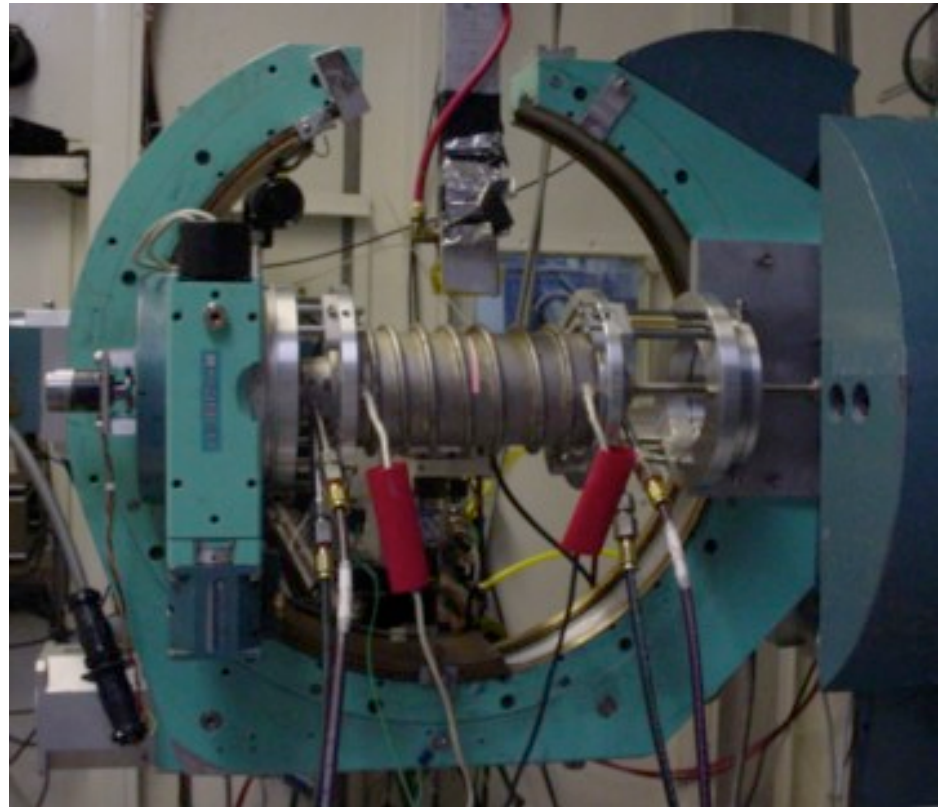
Howard et al. recently proposed a revised transition path for SrZrO₃

- Howard et al. have proposed a revised transition path based on:
 - neutron powder diffraction at HRPD (ISIS)
 - group theory analysis (Howard and Stokes)
- Comparison between the two paths
 - old path: Pnma ⇒ **Cmcm** ⇒ I4/mcm ⇒ Pm3m
 - new path: Pnma ⇒ **Imma** ⇒ I4/mcm ⇒ Pm3m
 - old path: $a^+b^-b^- \Rightarrow a^0b^+c^- \Rightarrow a^0a^0c^- \Rightarrow a^0a^0a^0$
 - new path: $a^+b^-b^- \Rightarrow a^0b^-b^- \Rightarrow a^0a^0c^- \Rightarrow a^0a^0a^0$
 - In the old path, the first and second transitions are discontinuous
 - In the new transition path, the first transformation is continuous
 - Howard constrained the Imma unit cell to be metrically tetragonal



The crystal structure of SrZrO_3 was studied using the Ames High Temperature Powder Diffraction Furnace at the NSLS X14A beamline

- Benefits of synchrotron radiation
 - High flux and resolution
 - Tunable wavelength
 - Monochromatic, parallel beam
- The Ames Furnace
 - Margulies, Kramer, et al. (Ames Lab)
 - Temperatures up to 1500 °C
 - Gas flow system
 - Capillary sample holder magnetically coupled to a motor for sample rotation
 - Improves particle statistics
 - Minimizes preferred-orientation effects

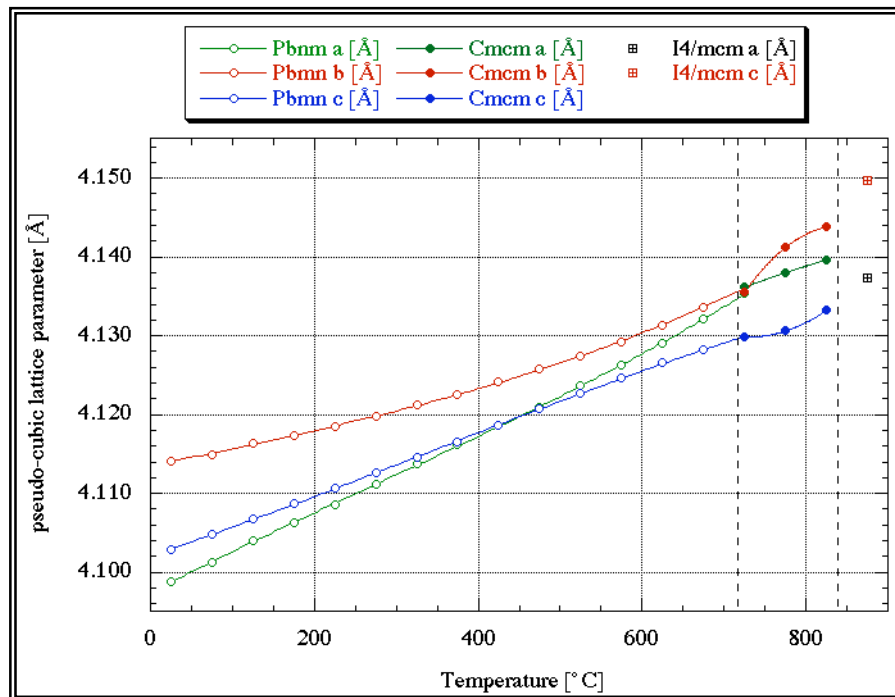


Diffraction patterns of SrZrO_3 were collected at 33 ± 1 , 735 ± 6 , 760 ± 7 , and 884 ± 10 °C (calibrated temps)

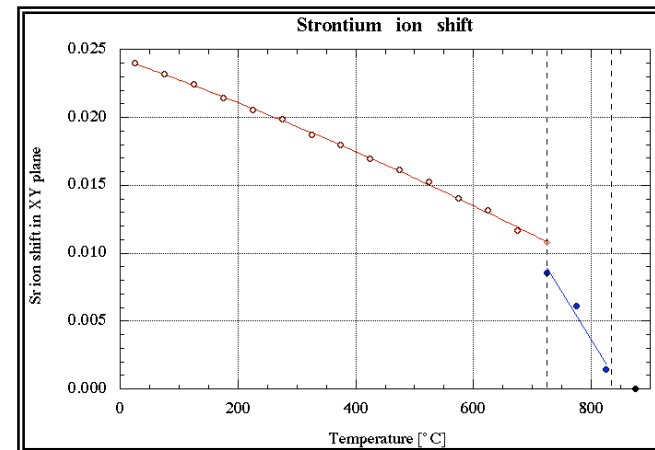
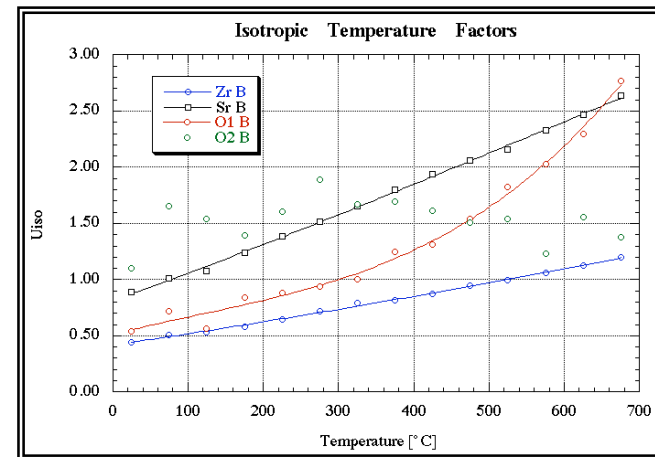


OAK RIDGE NATIONAL LABORATORY
U. S. DEPARTMENT OF ENERGY

With such high quality data we can determine accurate lattice parameters, atom positions and vibrations

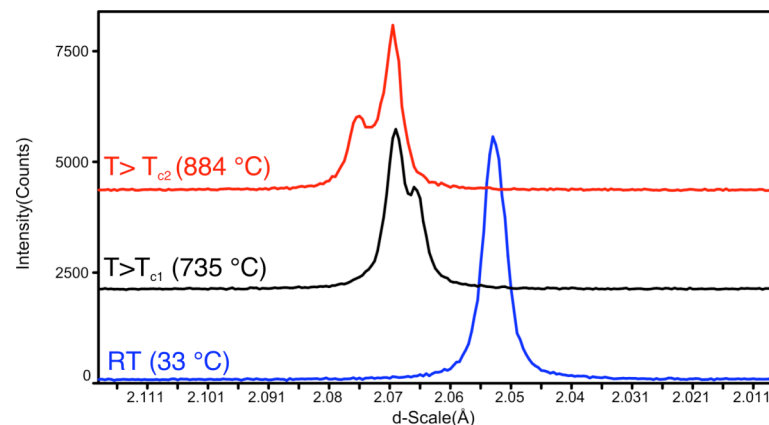
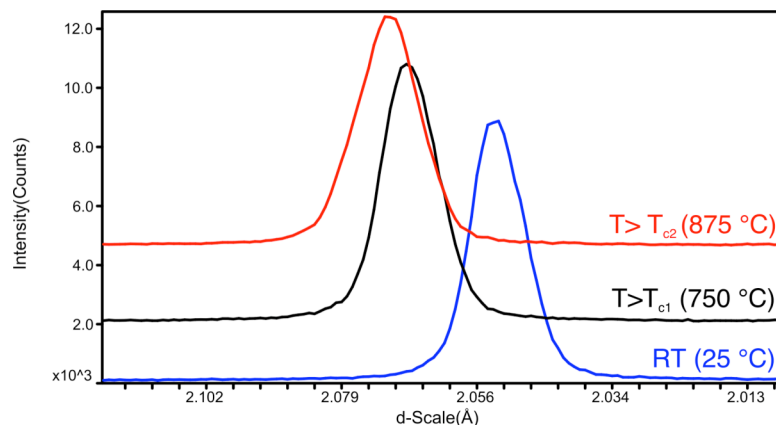


Note that this is a subtle transformation!
A more dramatic transformation is much easier to resolve.



High-resolution in-situ synchrotron data from X14A resolve ambiguities in in-situ laboratory XRD data

- With in-situ laboratory X-ray data (below, left), the {220} and {004} peaks cannot be resolved
 - This ambiguity enables multiple erroneous indexing schemes
- With in-situ, high resolution synchrotron data (below, right) these peaks are readily resolved
 - Structural variations not visible with laboratory facilities become observable with SXRD

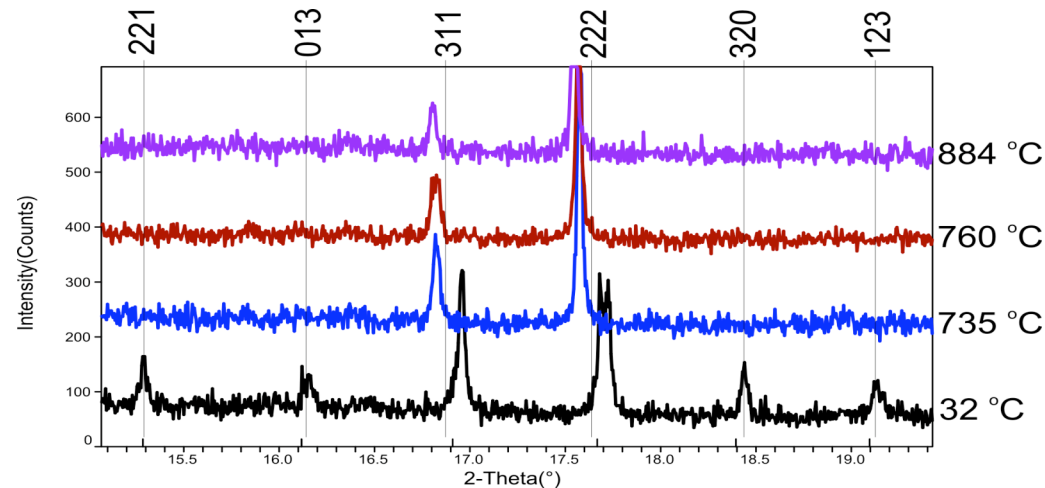


Three phases of SrZrO₃ observed with laboratory X-ray data (left) and synchrotron data (right).



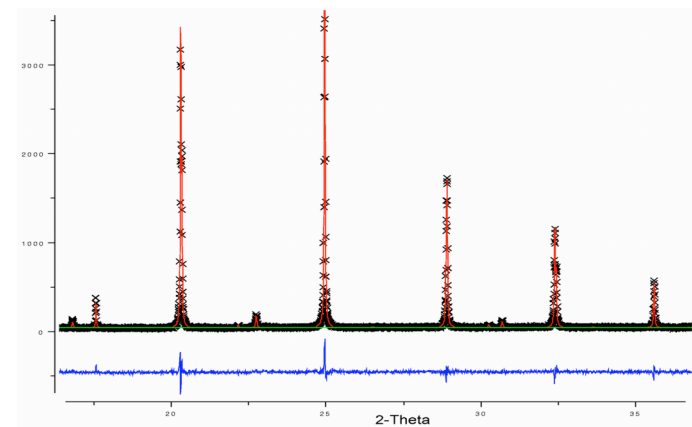
Superlattice reflections in X14A diffraction pattern differentiate between in-phase and antiphase octahedral tilting

- Superlattice peaks were indexed using a doubled cubic perovskite cell
 - Antiphase tilts produce peaks with all odd Miller indices.
 - In-phase tilts produce peaks with two odd and one even Miller indices
- At all temperatures (32, 735, 760, and 884 °C) antiphase tilts are present
 - At 32 °C, in-phase tilts are present
 - *At 735 and 760 °C, only antiphase tilts are present*
 - Consistent with the $Imma$ ($a^0b^-b^-$) space group, but not with $Cmcm$ ($a^0b^+c^-$)
 - SXRD data consistent with the neutron diffraction data of Howard et al.



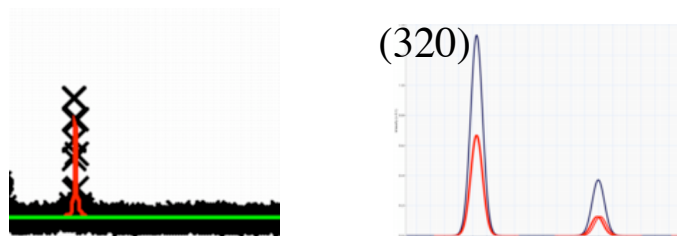
Refinement of the SrZrO₃ crystal structure in the Imma space group is good but some problems remain

- Rietveld refinement in Imma of the diffraction pattern collected at 735 °C
 - LP's 5.8536(2) x 8.26292(6) x 5.8525(2) Å
 - $X^2 = 1.63$, $wRp = 14.65\%$
 - Not metrically tetragonal ($a/c = 1.0002$)
 - Peak profile and lattice parameters are correlated
- Refinement in the Cmcm space group
 - $X^2 = 1.62$, $wRp = 14.59\%$, ~ equivalent fit
 - Oxygen atoms moved to positions equivalent to those in Imma
- No other space group (R3c, etc.) satisfactorily describes the diffraction data



Computer simulation in the $Im\bar{m}a$ space group indicates that the unit cell is indeed nearly metrically tetragonal ($a \approx c$)

- Empirical potential models used to simulate the $SrZrO_3$ crystal structures
 - GULP code of J. Gale, Imperial College
- Simulation of the $Im\bar{m}a$ crystal structure of $SrZrO_3$
 - Produces an a/c ratio of 1.00012
 - Compares favorably with the a/c value of 1.0002 from Rietveld refinement
 - The ratio a/c is very nearly unity because of balancing interatomic forces
 - The unit cell parameters are nearly equal because of nearly equivalent interatomic forces in those directions
 - Simulation of the $Cmcm$ space group shows that the intensity of peaks from in-phase tilting are not negligible

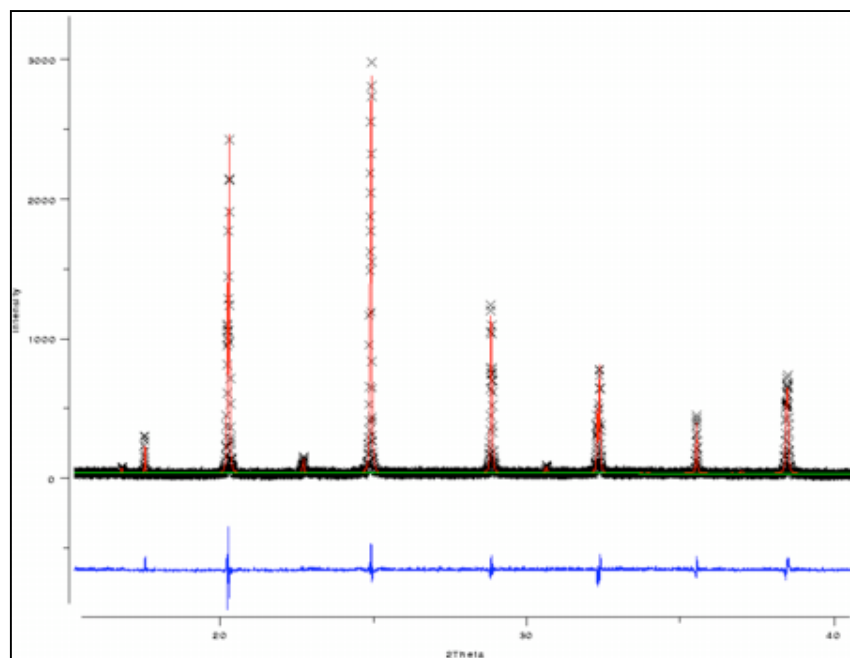


Comparison of calculated diffraction patterns from computer simulation results. On the left is the experimental data (black) and the calculated pattern for $Im\bar{m}a$ (red). On the right is the calculated pattern for $Cmcm$ - Note the relatively strong (320) peak that is not observed in the experimental data.



Data collected at 884 °C refined well in the I4/mcm space group

- Data from synchrotron are consistent with the previous reports
 - Refinement in the I4/mcm space group yields $X^2 = 1.77$
 - Lattice parameters are $5.85399(3) \times 8.30120(7) \text{ \AA}$



OAK RIDGE NATIONAL LABORATORY
U. S. DEPARTMENT OF ENERGY

SrZrO₃ Conclusions

- At room temperature, SrZrO₃ has both antiphase and in-phase octahedral tilting
 - The data are consistent with the Pnma space group
- Above the transition temperature at 727 °C, only antiphase octahedral tilting is present
 - The best space group for refinement is Imma
 - Correlation between lattice parameters and peak shape profiles impedes crystal structure refinement
 - Empirical potential models support the application of the Imma space group
- Above 832 °C, SrZrO₃ is tetragonal with only antiphase tilting
 - The data are consistent with the I4/mcm space group



- **The Diffraction and Thermophysical Properties Group**
- **X14A PRT and Facilities**
- **Examples of Other Studies at X14A**



There are four integrated and overlapping focus areas within the DTP Group at ORNL

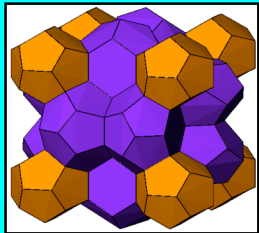
- **Crystal Chemistry and Diffraction**
 - x-ray, synchrotron, neutron facilities and expertise
 - RT, in situ and real time options
- **Residual Stress**
 - x-ray, synchrotron, neutron facilities and expertise
 - applied loads, elevated temperature, environmental effects
 - range of specimen dimensions (100 Å thick to ~1 m)
- **Thermography and Thermophysical Properties**
 - thermal analysis and thermal transport properties
 - IR thermography (expanding)
 - radiative properties (new)
- **Engineered Microstructures & Property Development**
 - processing in high magnetic fields
 - heat treating and process technology



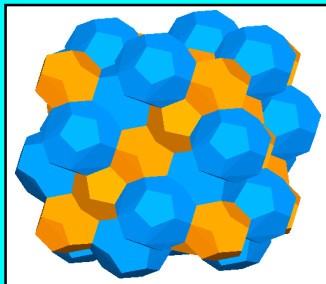
Crystal Chemistry & Diffraction: Developing new materials and understanding

HTML-DUC

Carbon Sequestration

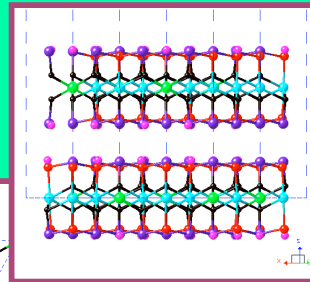
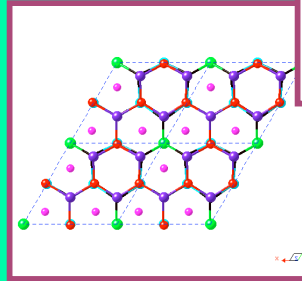


Clathrate
Structure I
 $X_8(\text{H}_2\text{O})_{46}$
 $X = \text{CH}_4, \text{CO}_2, \text{C}_2\text{H}_6$

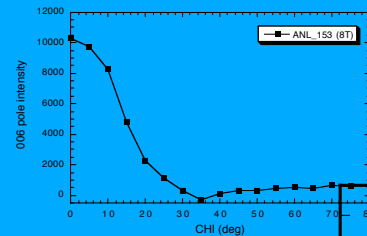
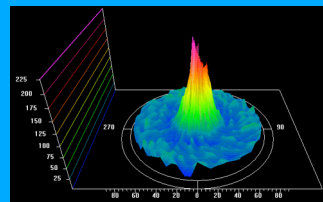


Clathrate
Structure II
 $X_{24}(\text{H}_2\text{O})_{136}$
 $X = \text{N}_2, \text{O}_2, \text{C}_3\text{H}_8$

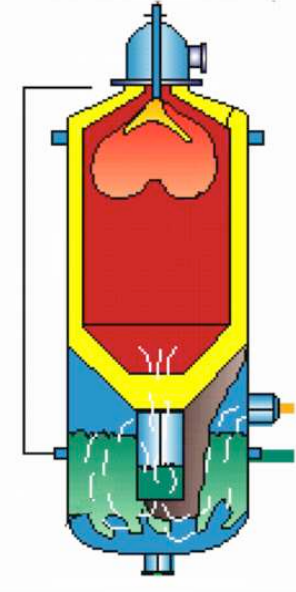
Oxygen Ion Conductors



Doped
Bismuth
Oxides



Permanent Magnets



Containment for
BL Gasification
Environment

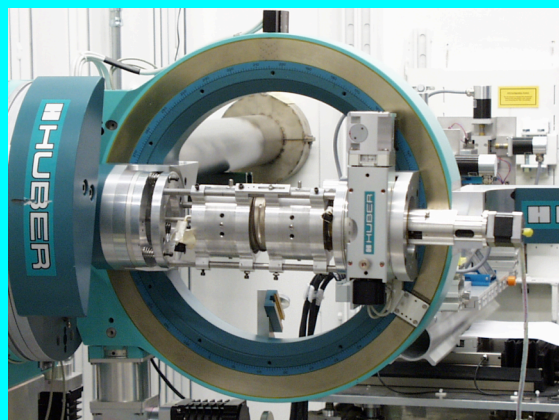
Structural and in-situ information leads to novel ideas and to the development of new materials and applications.



OAK RIDGE NATIONAL LABORATORY
U. S. DEPARTMENT OF ENERGY

In-situ, real-time studies by X-ray and neutron diffraction are key to crystal chemistry advances

**Synchrotron HTXRD
to 1600°C (1 atm)**



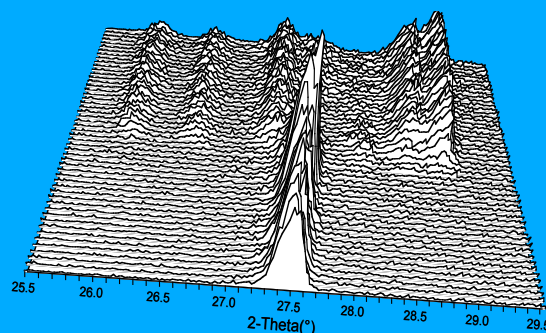
**Laboratory XRD
to 1500°C (1 atm) or
2300°C (vac)**



**Neutron Diff. to
1800°C in air/vac**



The temperature, atmosphere, and pressure play an important role in many structure-property relationships



Pressure cells



Data understanding increasingly will use thermochemical and atomistic modeling



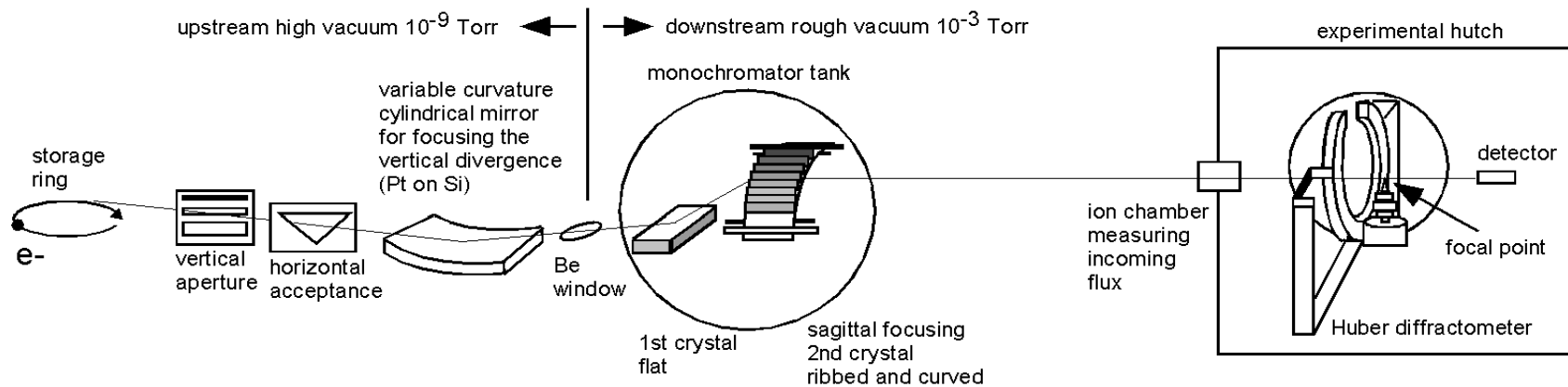
**OAK RIDGE NATIONAL LAB
U. S. DEPARTMENT OF ENERGY**

Current X14A Beamline PRT Members

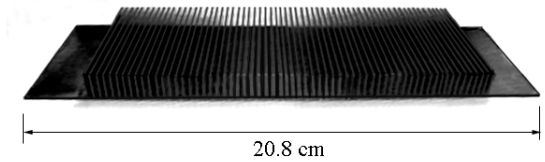
- PRT Spokesperson
 - C. R. Hubbard (ORNL-M&C)
- PRT Local Contact/Beamline Scientist
 - J. Bai - Local contact (Univ. of Tennessee)
- PRT Members
 - J. Biernacki (Tennessee Tech Univ.)
 - T.R. Watkins (ORNL-M&C)
 - E.A. Payzant (ORNL-M&C)
 - C.J. Rawn (ORNL-M&C & Univ. of Tennessee)
- PRT Collaborators/Frequent General Users
 - P. Dutka (Northwestern)
 - S. Moss (U. of Houston)
 - T. Tyson (NJIT)



1999 upgrades continue to provide superior optics, excellent flux and improved operation!



- High performance grazing incidence mirror
- Flat Si (111) monochromator (H₂O cooled)
- Sagittal focussing Si (111) monochromator



Energy range with mirror 3.5 – 26 keV
 Beam divergence $V < 0.03^\circ$, $H = 0$ to 0.6°
 Energy resolution with mono. < 3 eV

Flux approaching NSLS insertion devices



OAK RIDGE NATIONAL LABORATORY
 U. S. DEPARTMENT OF ENERGY

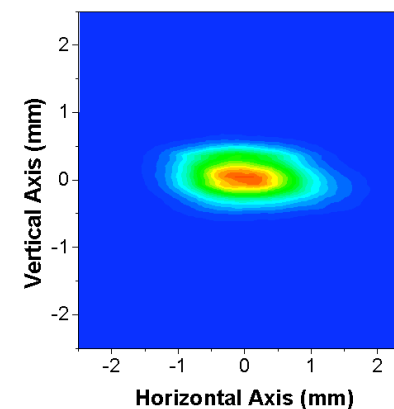
Capabilities of Beamline X14A

- **Sagittal Focusing Monochromator with 10 mrad Horizontal Acceptance and A Cylindrical Pt/Si Vertically Focusing Mirror**

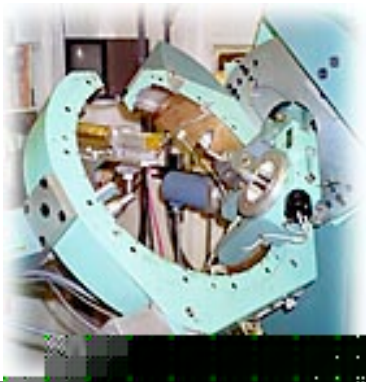
High flux: 3×10^{12} photon/sec/200mA at 8.0 keV

7×10^{11} photon/sec/200mA at 17.0 keV

Focused Beam Size: 0.5 mm x 1.25 mm (FWHM)



Flexible Focusing Mechanism: The vertical and horizontal focusing can be conducted independently, ideal for diffraction in liquid surface.



Huber 6-circle Diffractometer with Eulerian cradle 513 has a gap in the chi-circle, allowing wider sample observation range.

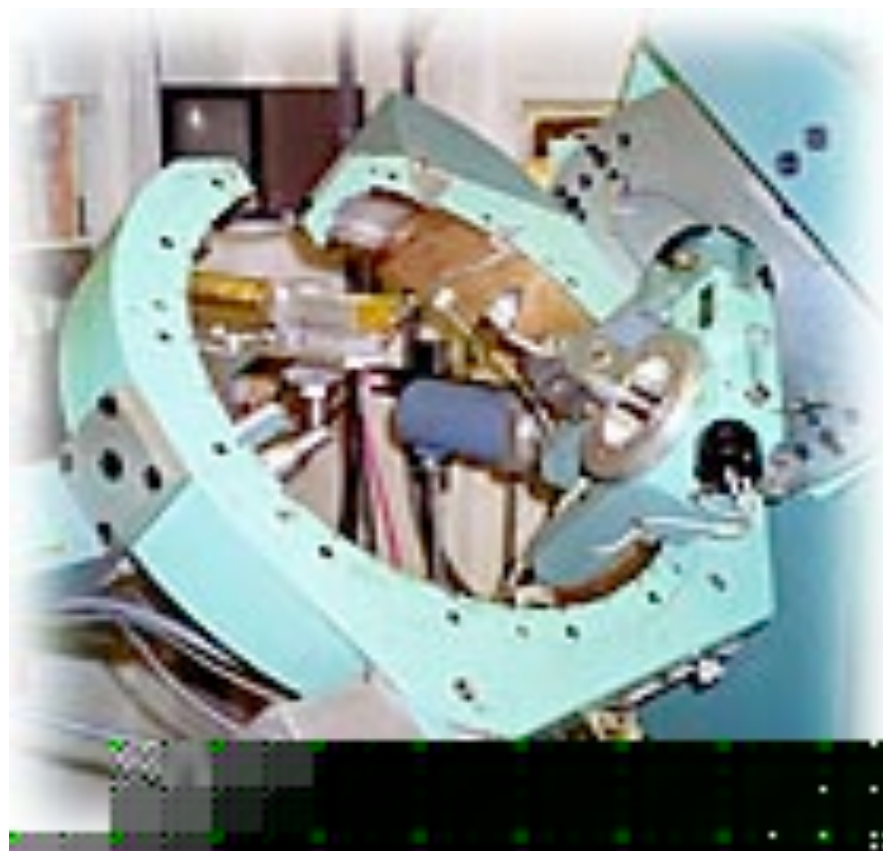


OAK RIDGE NATIONAL LABORATORY
U.S. DEPARTMENT OF ENERGY

X14A's Six-Circle Huber Goniometer Provides Excellent Flexibility

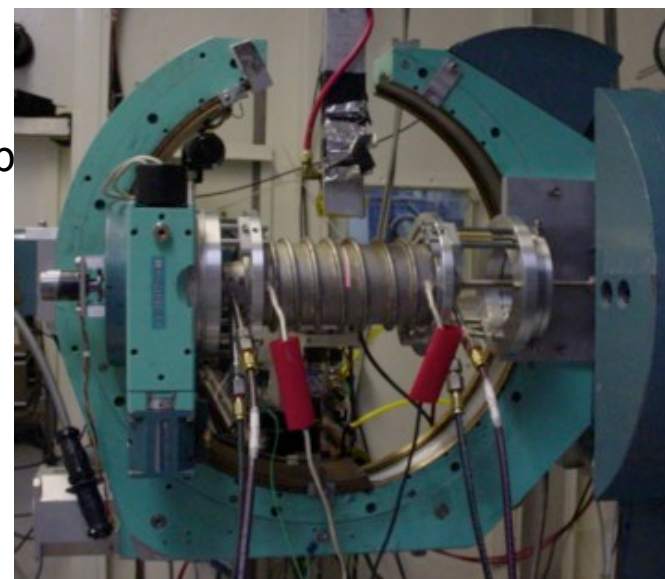
Accessories at X14A

- **Capillary furnace (FY01)**
 - Rotating specimen
 - Gas flow option
 - Uniform heating
- **HT Buehler stage**
 - 1500°C in 1 atm
 - ~2400°C in vacuum
- **Be dome hot stage**
 - 700°C in vacuum
- **Displex closed cycle cryostat**
- **Ge & graphite analyzer crystals**
- **Remote collaboration tools**
<http://www.ornl.gov/doe2k/hfir/>



2001-2004 Major Additions and Upgrades

- **Capillary furnace added for in situ diffraction**
 - Designed and built for X14A by Matt Kramer, Ames Lab
 - Heats sample up to 1500°C
 - Gas flow system
 - Rotating capillary
- **Upgrades**
 - Software: SPEC, Jade, Shadow, GSAS ...
 - Database: ICDD-PDF (yearly update)
 - UNIX Workstation, Motor controller, vacuum pumps, ...
 - Electronic notebook and video presence
- **Development Efforts**
 - Collaborated with NSLS on Banana Detector
 - Proposal to DOE (led by P. Stephens)
 - Speaker at several NSLS Workshops



HTML User Program:

www.html.ornl.gov



OAK RIDGE NATIONAL LABORATORY
U.S. DEPARTMENT OF ENERGY

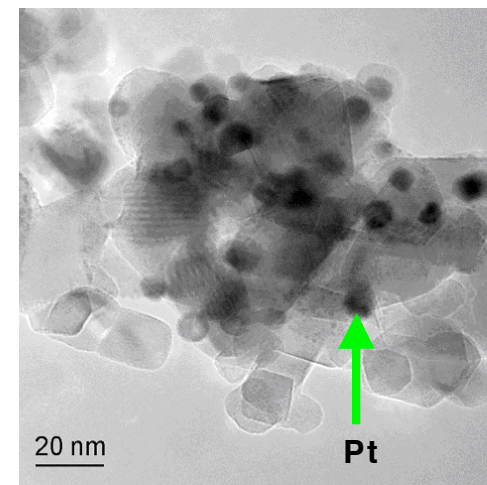
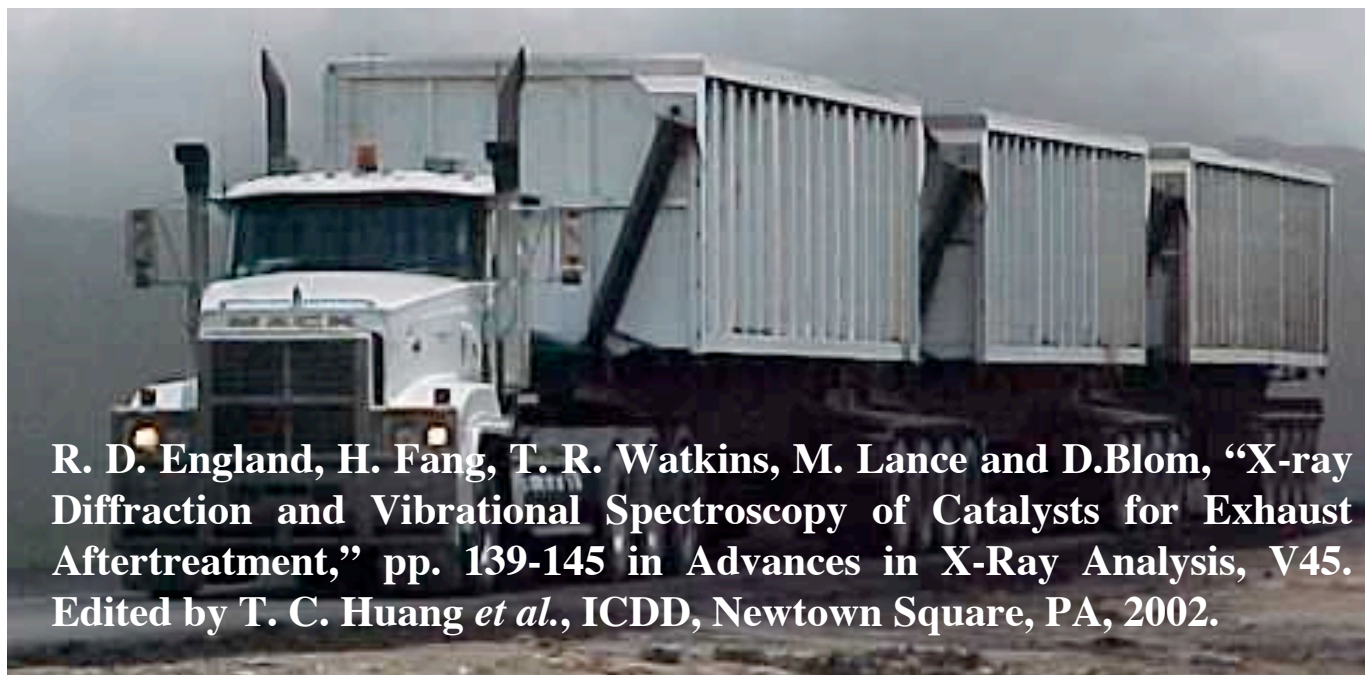
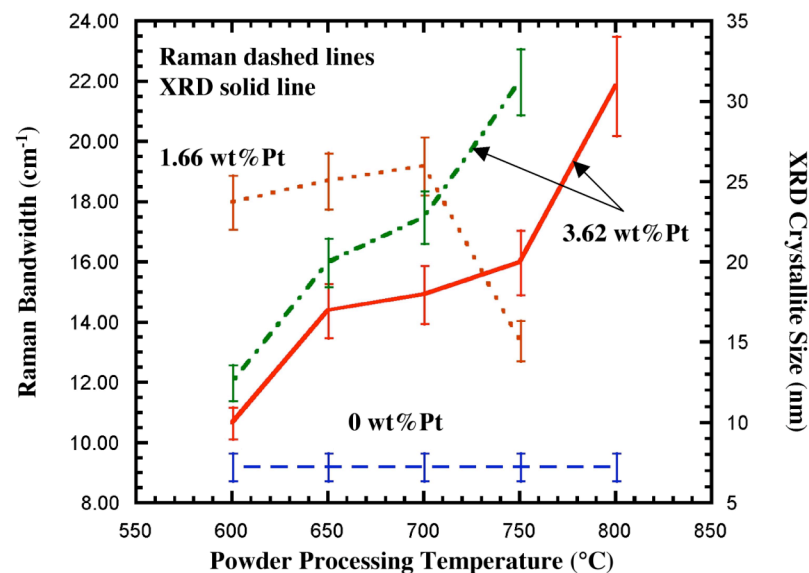
Example of Other Scattering Studies at X14A

- **Crystallite size**
- **Residual stress**
 - elevated temperature, curved surfaces, small areas
- **GIXD for structure at surfaces**
- **High resolution x-ray emission - electronic state of Mn**
- **Reciprocal space mapping - order parameters**
- **Resonant x-ray scattering**



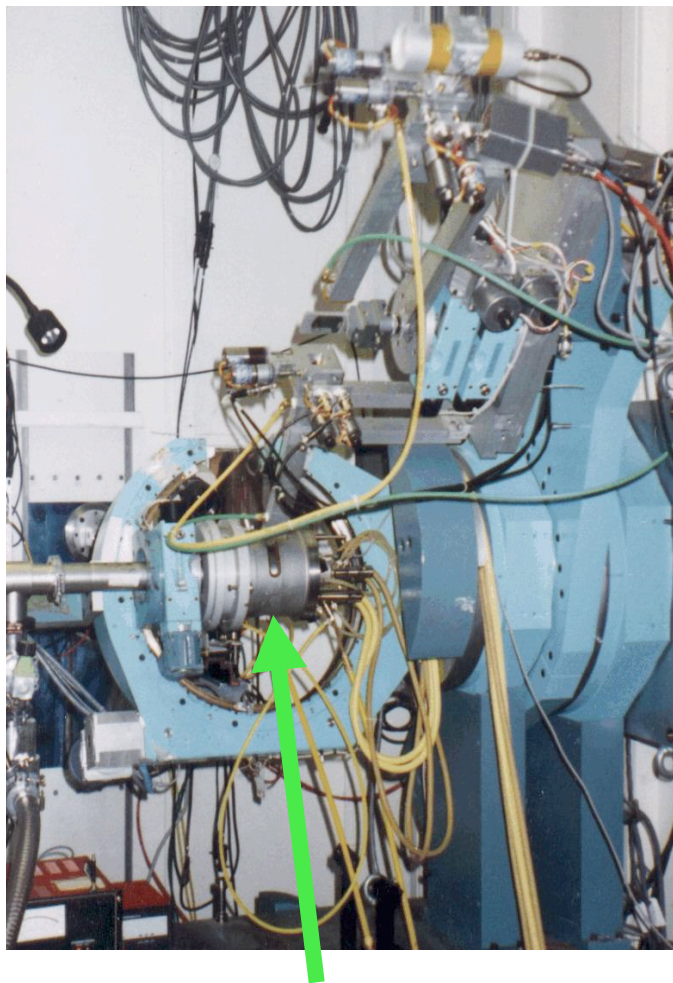
Catalyst characterization - T.R. Watkins (ORNL)

- Goal: To meet 2007 diesel engine emission requirements
- Catalytic activity decreases with surface area \Rightarrow Platinum (Pt) particle size increases
- X-ray diffraction, Raman & TEM techniques track Pt size change
- Collaboration: HTML/ORNL & Cummins Engine



Parallel beam optics for residual stress studies

T.R. Watkins (ORNL)



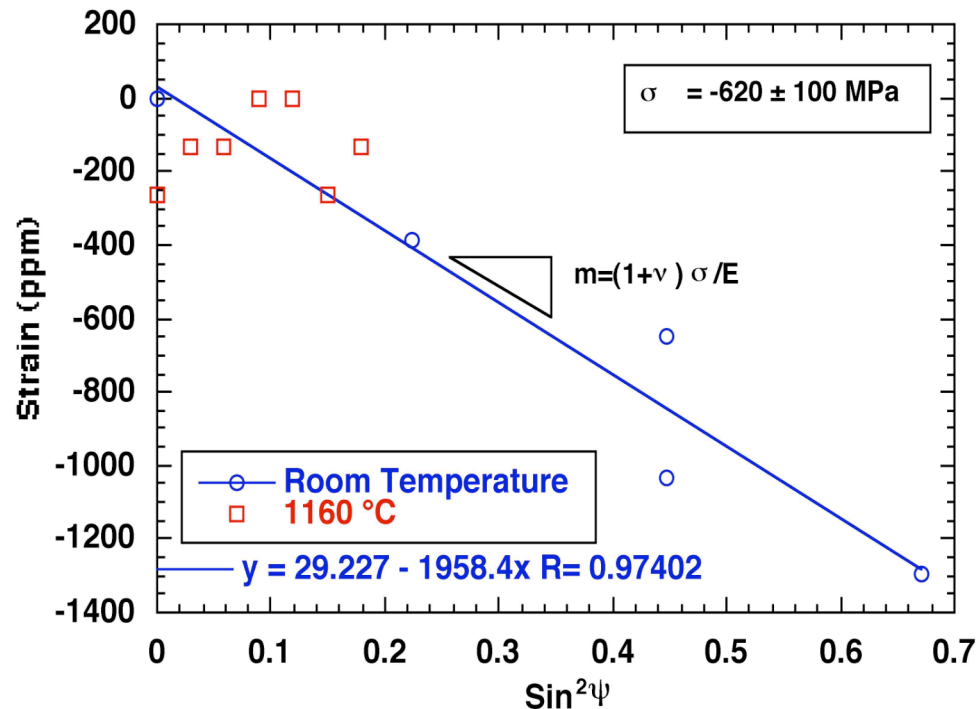
- **Significantly improves the quality of residual stress data by dramatically reducing the sample surface displacement effect on peak position**
 - Increases confidence in data interpretation
 - **HTXRD stress (CTE shift eliminated)**
 - **Invaluable for curved surfaces**
- **Example: Thermal barrier coatings (TBCs)**
 - Prolong the life of metallic components
 - TBC failure: spallation of the top coat due to oxide scale growth at the bond coat/top coat interface
 - Understanding the residual stresses of the oxide scale growth is critical to enhancing the performance and reliability of TBC systems.

Buehler HDK 2.3 HT
stage on X14A



OAK RIDGE NATIONAL LABORATORY
U. S. DEPARTMENT OF ENERGY

In-situ oxidation of bare bond coat: Little residual strain present at 1160°C



- X14A synchrotron radiation ($\lambda = 1.537$ Å)
- (300) Al_2O_3 , $\sim 67.9^\circ 2\theta$
- HT residual stress similar to others*
- RT stress is 1/3 in magnitude to those reported due to partial spallation or cracking‡

* M. Groß et al., Adv. X-Ray Anal., V. 42

‡ C. Sarioglu et al., Oxidation of Metals, 1997

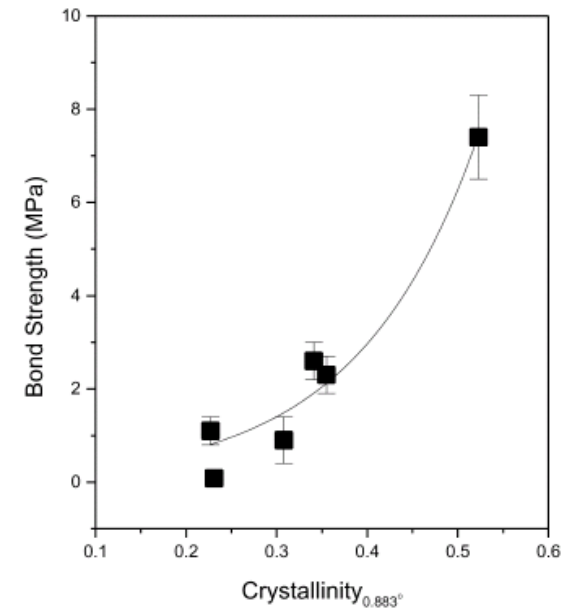
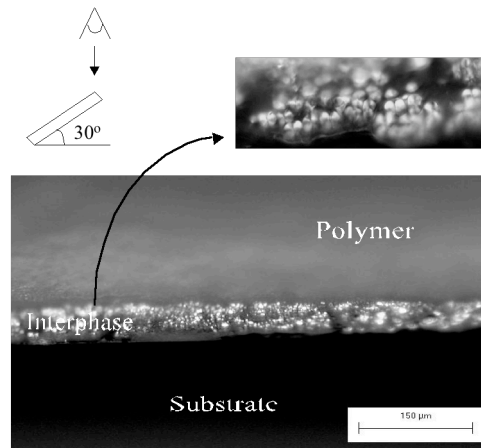
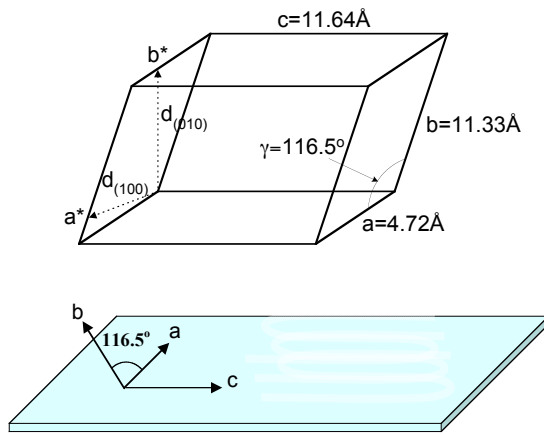
Publication: T. R. Watkins, O. B. Cavin, J. Bai and J. A. Chediak, "Residual Stress Determinations Using Parallel Beam Optics," pp. 119-129 in Advances in X-Ray Analysis, Vol. 46. Edited by T. C. Huang *et al.*, ICDD, Newtown Square, PA, 2003.



OAK RIDGE NATIONAL LABORATORY
U. S. DEPARTMENT OF ENERGY

Grazing Incidence X-ray Diffraction Studies on the Structures of Polyurethane Films and Their Effects on Adhesion to Al Substrates

Jangsoon Kim and Earle R. Ryba (The Pennsylvania State University)



The bond strength of the polyurethane film to the aluminum was found to be exponentially proportional to the crystallinity including the crystalline interphase formed near the substrate. It is also found that the polymer film contained more (100) planes and provided higher bond strength. Aging led to the improvement of bulk crystallinity of all the samples and dramatically increase the bond strength.

Publication: J. Kim et al., Polymer 44 (2003) 6663–6674



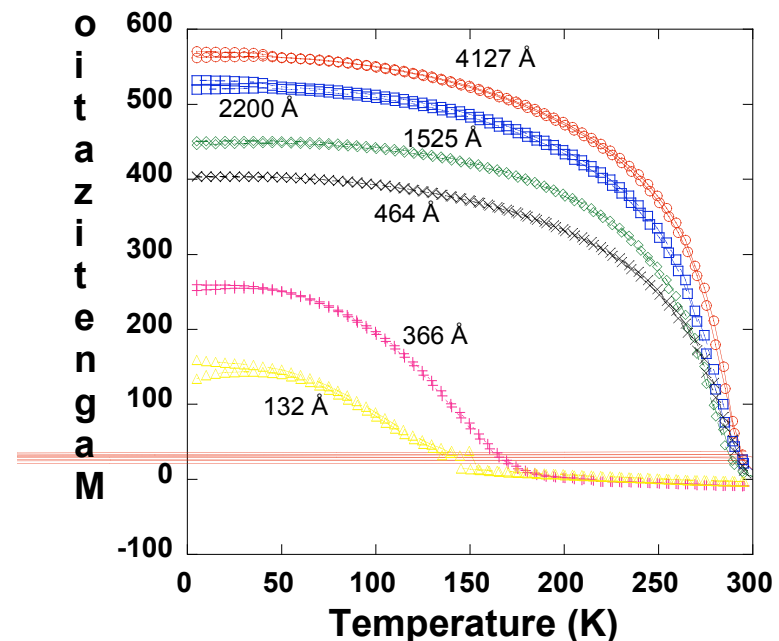
OAK RIDGE NATIONAL LABORATORY
U.S. DEPARTMENT OF ENERGY

Observation of a Strain Induced High-Spin to Low-Spin Transition in Thin Manganite Films

Q. Qian, T. A. Tyson (NJIT) , J. Bai (ORNL) and M. DeLeon (NJIT)

In order to understand the observed dramatic reduction in magnetization with decrease in manganite film thickness, high resolution Mn K_{β} x-ray emission measurements were conducted on films with thickness ranging from 50 to 4000 Å. The High flux available at X14A (10^{12} photons/sec) made this experiments on thin films possible. This work followed detailed x-ray diffraction studies on a broad range of manganite films. Evidence for strain induced high spin to low spin transition on the Mn sites was found. The resulting violation of the assumed strong Hund's rule coupling on the Mn sites suggest that the existing theoretical models of these correlated systems must be extended.

(
La_{0.8}MnO₃ Film Magnetization Curves

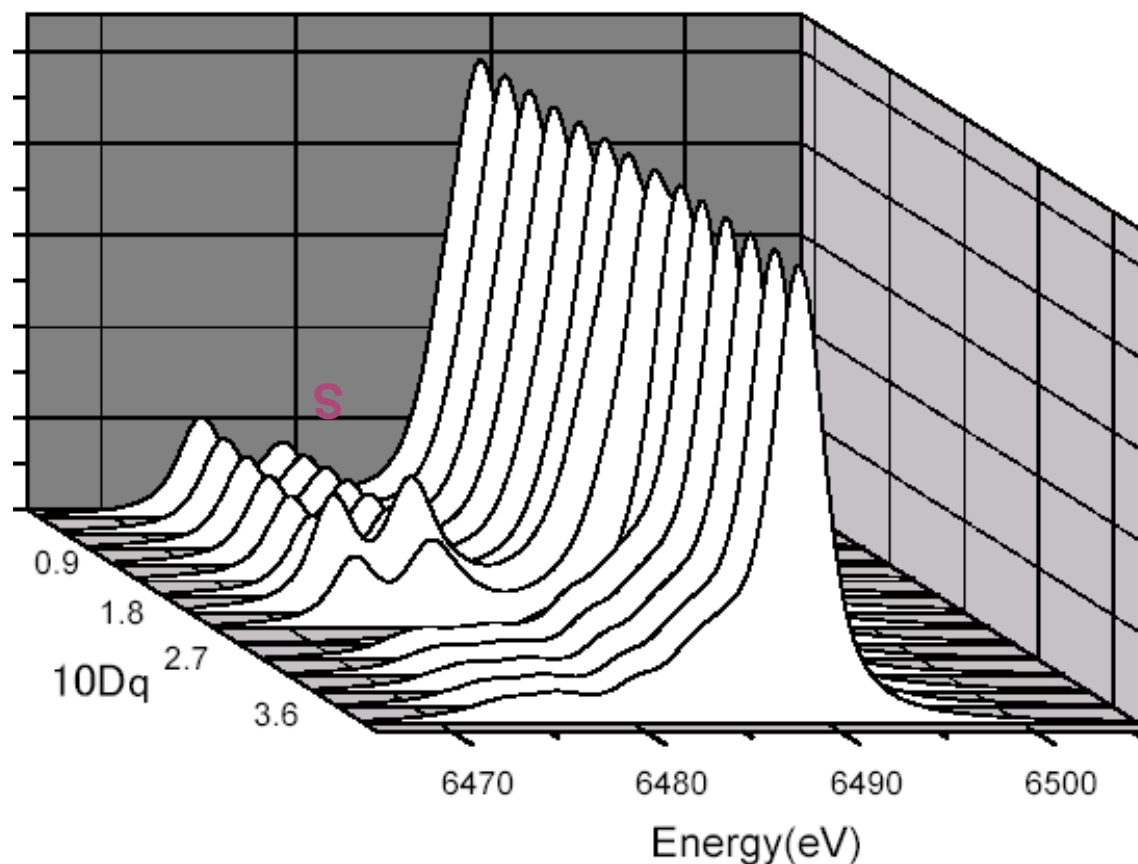


The magnetic moment per moment drops dramatically as the film thickness is reduced. The reduction had been attributed to spin canting or ferromagnetic-antiferromagnetic phase separation.



OAK RIDGE NATIONAL LABORATORY
U. S. DEPARTMENT OF ENERGY

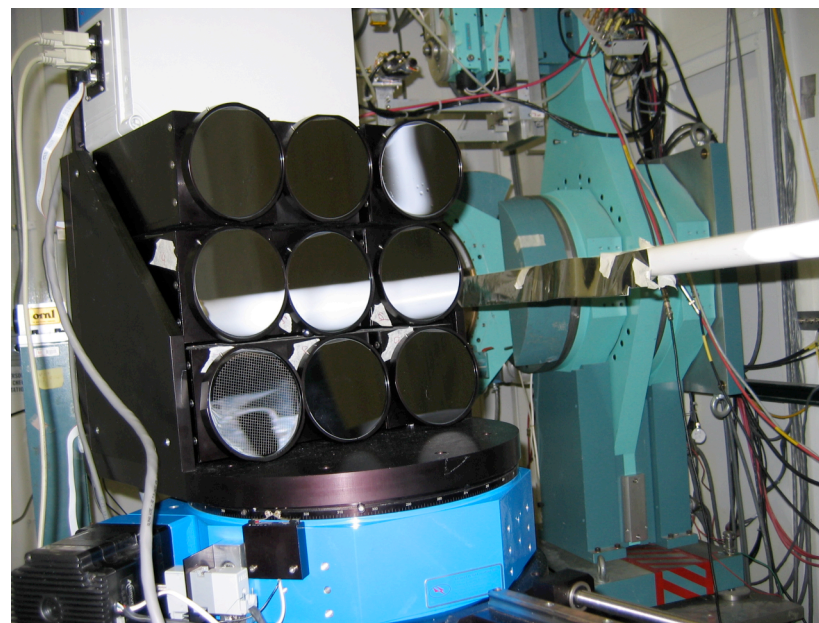
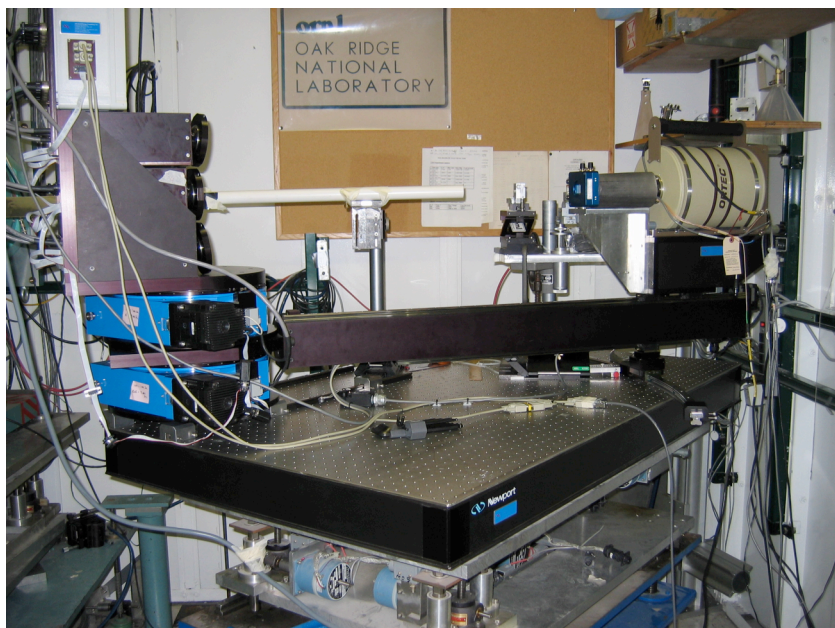
Calculated Mn^{3+} K_{β} Emission vs. $10Dq$



Simulation of Mn^{3+} K_{β} emission spectrum for varying $10Dq$ (e_g-t_{2g} splitting). Note the drop in the satellite features (S) for $10Dq$ above ~ 2.7 eV signifying the onset of the high-spin to low-spin transition on Mn.



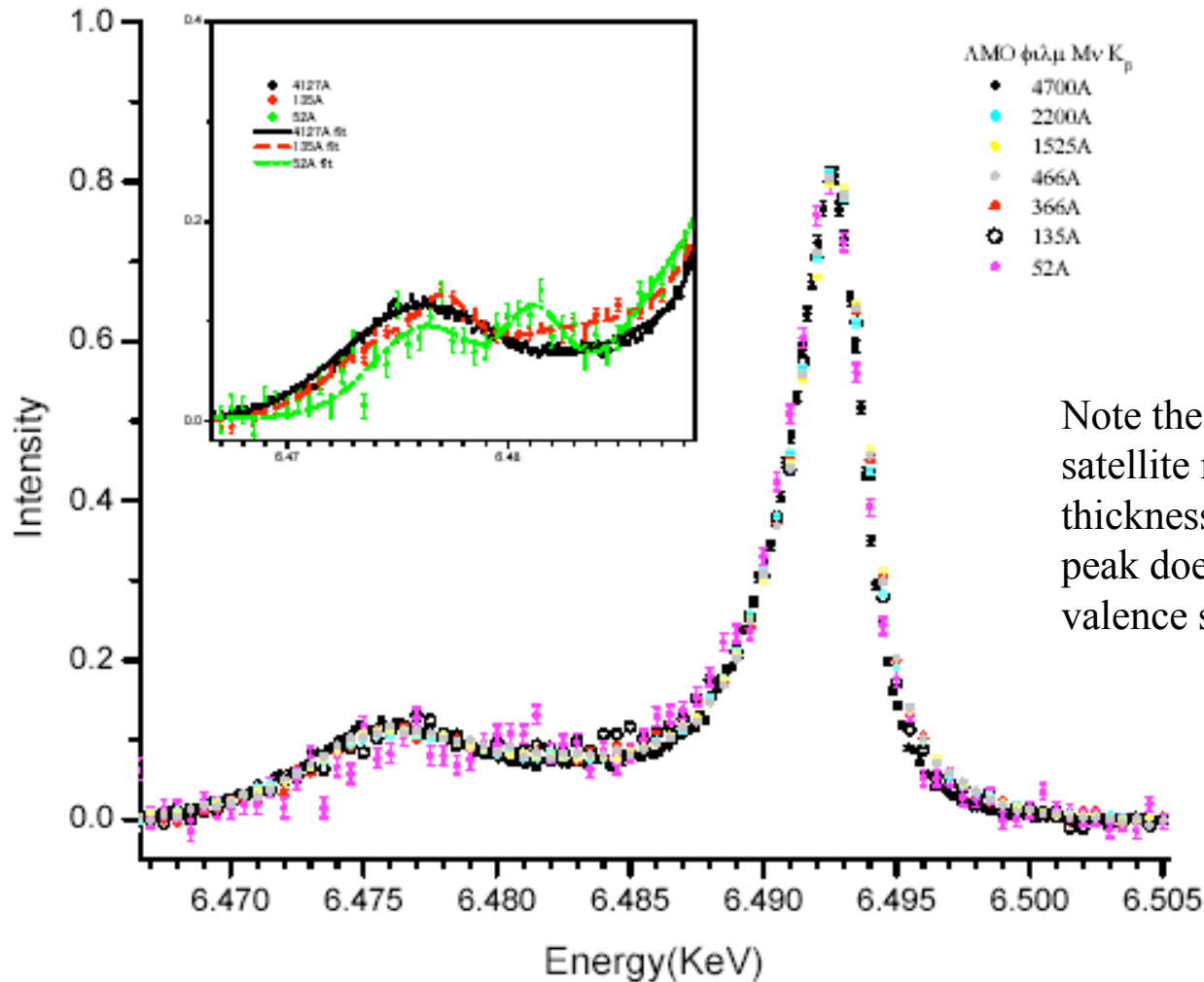
High Resolution X-Ray Spectrometer for Inelastic X-Ray Scattering Set up at X14A



A recently developed multi-mirror high-resolution x-ray analyzer system was used to conduct Mn K_{β} x-ray emission experiments on magnetic oxide films ranging from 52 to 4127 Å. On the left we show the full system comprised of a detector, sample support (next to detector) and the nine-element mirror system. The sample, detector and mirrors sit on a Rowland circle. On the right we show a blow-up of the full analyzer array. Each mirror can be adjusted independently in the horizontal and vertical planes with microradian precision. The high flux available at the beamline ($\sim 10^{12}$ photons/s in $1 \times 1 \text{ mm}^2$) makes possible these low cross-section experiments.



Measured Mn K_{β} Emission Spectra



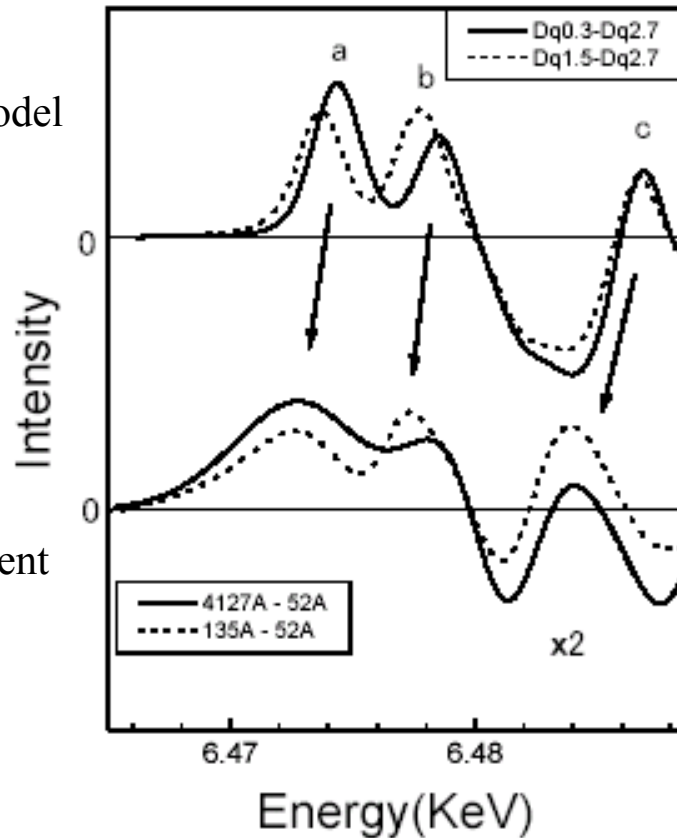
Note the reduction in intensity in the satellite region (inset) with reduced thickness. On the other hand, the main peak does not shift indicating a constant valence state



Difference Spectra

Mn³⁺ Model

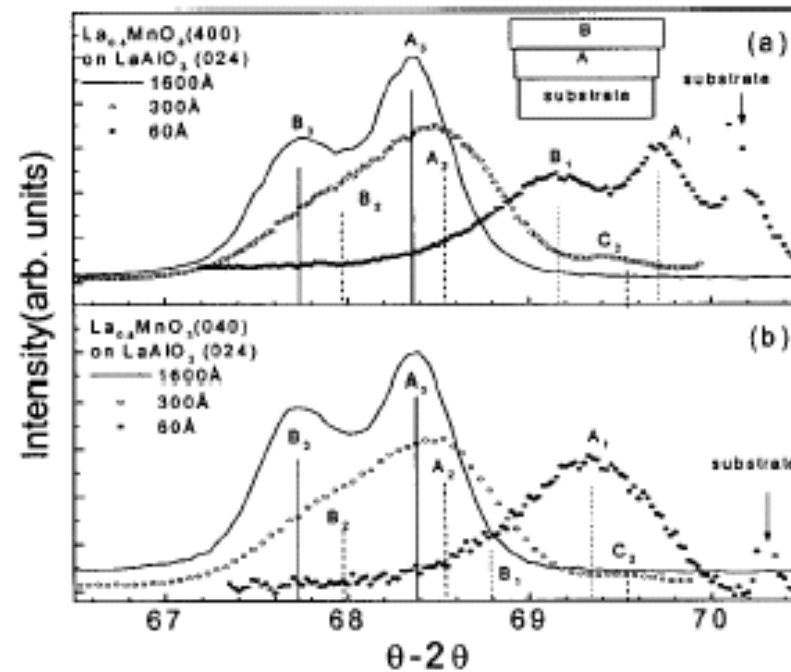
Experiment



Taking the differences between the high-spin and low-spin theoretical spectra (upper curves) and between the thick and the thin measured spectra (lower curves) reveals that indeed the highly strained thin films do exhibit a high spin to low spin transition.



In-Plane XRD Measurements on First Series Films



High Resolution In-plane $\{(400) \text{ and } (040)\}$ combined with out-of-plane reflections reveal a heavily strained layer near the substrate and relaxed layers far from the substrate.



Summary for Full Range of Films Studied

- **Very high strain induced by the substrate results in high-spin to low-spin Mn site transitions in manganite films. (The crystal field energy dominated over the Hund's exchange energy)**
- **Detailed x-ray diffraction measurements revealed multiple components in these films with a highly strained layer near the substrate.**
- **Work on both the La_xMnO_3 and the $\text{Nd}_{1/2}\text{Sr}_{1/2}\text{MnO}_3$ series reveals significant in-plane strain persisting beyond 2000 Å.**

Submitted and Published Work Based on X14A Experiments

- Q. Qian, T. A. Tyson, M. Deleon, C.-C. Kao, W. Prellier, J. Bai, A. Frenkel, A. Biswas and R. L. Greene, "Influence of strain on the Local Atomic, Electronic and Magnetic Structure of Manganite Films", Submitted to Phys. Rev. B.
- Q. Qian, T. A. Tyson, C. Dubourdieu, A. Bossak, J. P. Senateur, M. Deleon, J. Bai, and G. Bonfait, "Structural studies of annealed ultrathin $\text{La}_{0.8}\text{MnO}_3$ films", Applied Physics Letters **80**, 2663 (2002).
- Q. Qian, T. A. Tyson, C. Dubourdieu, A. Bossak, J. P. Senateur, M. Deleon, J. Bai, G. Bonfait, and J. Maria, "Structural, magnetic, and transport studies of $\text{La}_{0.8}\text{MnO}_3$ films", Journal of Applied Physics **92**, 4518 (2002).
- Q. Qian, T. A. Tyson, C. C. Kao, W. Prellier, J. Bai, A. Biswas, and R. L. Greene, "Strain-induced local distortions and orbital ordering in $\text{Nd}_{0.5}\text{Sr}_{0.5}\text{MnO}_3$ manganite films", Physical Review B: Condensed Matter and Materials Physics **63**, 224424/1 (2001).



X-ray Studies of Spontaneous Atomic Ordering in III-V Semiconductor Alloy Films

UH

S. Moss and J.H. Li, Univ. of Houston

Information obtained from SXRD quantitative analysis:

1. Two variants coexistence
2. Order parameter
3. Atomic displacement
4. Anti-phase boundaries
5. Orientational (variant) boundaries
6. Size and spatial distribution of the antiphase and the orientational boundaries

J.H. Li, "X-ray characterization of CuPt-ordered semiconductor alloy films," in *Spontaneous Ordering in Semiconductor Alloys*, ed. A. Mascarenhas (Plenum Press/Kluwer Academic, 2002)



OAK RIDGE NATIONAL LABORATORY
U. S. DEPARTMENT OF ENERGY

Determination of the Order Parameter

- Traditional method

$$I_{\text{fundamental}} \propto |F_{\text{fundamental}}|^2$$

$$I_{\text{order}} \propto s^2 \cdot |F_{\text{order}}|^2$$

$$s \propto I_{\text{order}} / I_{\text{fundamental}}$$

Problems:

Modulation of the ordering reflection by atomic displacement and possibly also by antiphase domains.

Determination of the intensity of a fundamental reflection is often not easy because the layer is usually lattice matched to the substrate.

In case of co-existence of two variants, one effectively determines the product of the order parameter and the volume fraction of the corresponding variant.



Determination of the Order Parameter

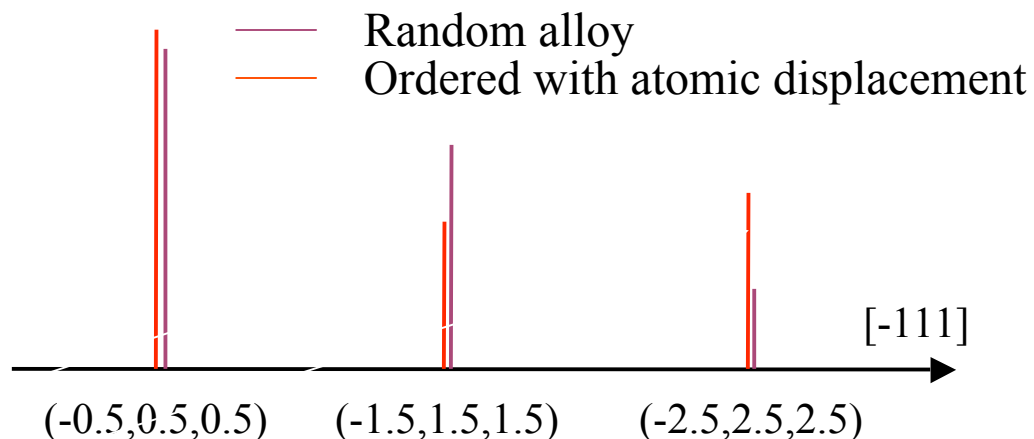
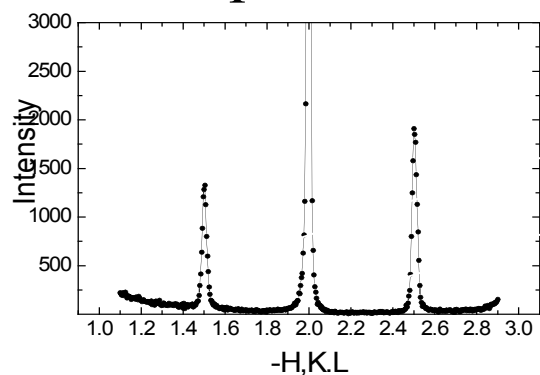
Our Approach

J. H. Li, R. L. Forrest, S. C. Moss, Y. Zhang, A. Mascarenhas, J. Bai, "Determination of the order parameter of CuPt-B ordered GaInP₂ films by x-ray diffraction," Journal of Applied Physics, Volume 91, Issue 11, pp. 9039-9042, 1 June 2002



- ✓ No structural detail is needed
- ✓ Average order parameter for all ordered domains of the same variant

Experiment



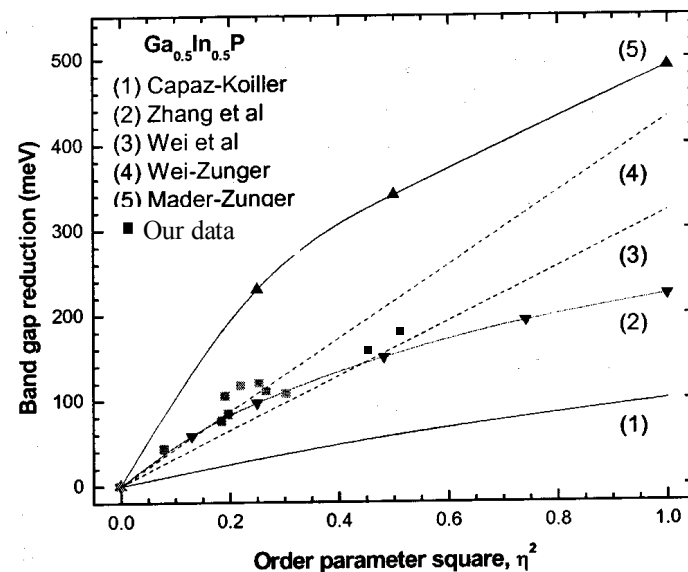
$$\text{Amplitude of intensity modulation} \propto |\mathbf{Q} \cdot \delta|^2$$



Impact of atomic ordering on physical properties of III-V semiconductors - J.H. Li, U. of Houston

- Electronic band-gap reduction, up to ~ 100 meV
- Valance band splitting
- Effective mass anisotropy
- Electron spin polarization

•
•
•

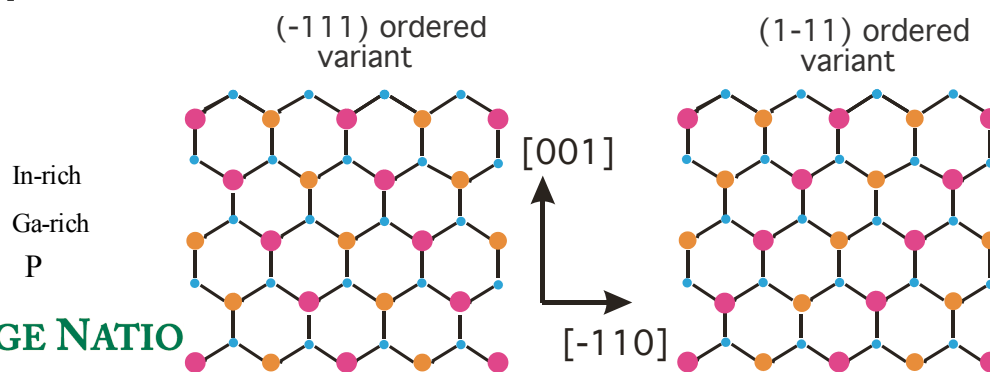
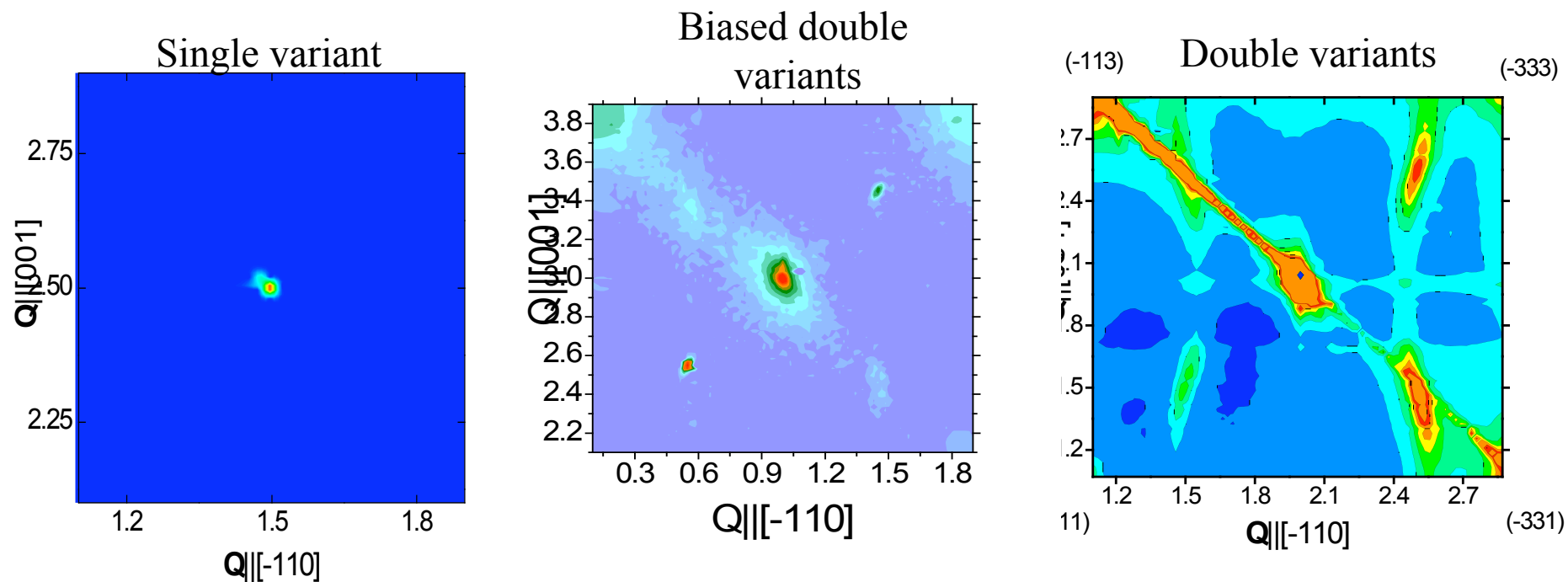


Theoretical models of atomic ordering on band gap reduction.

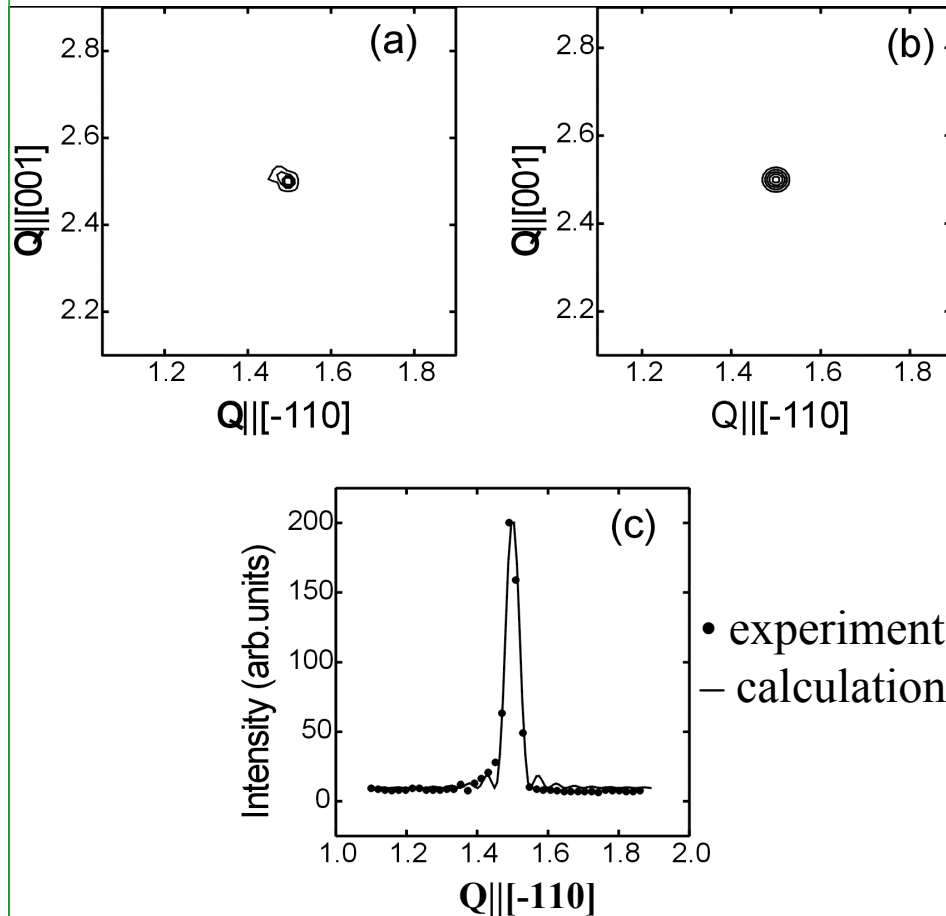
Clearly, determination of order parameter is crucial for development of appropriate theory and device applications



X-ray [110] Zone Diffraction - Ga_{0.5}In_{0.5}P/GaAs (001)



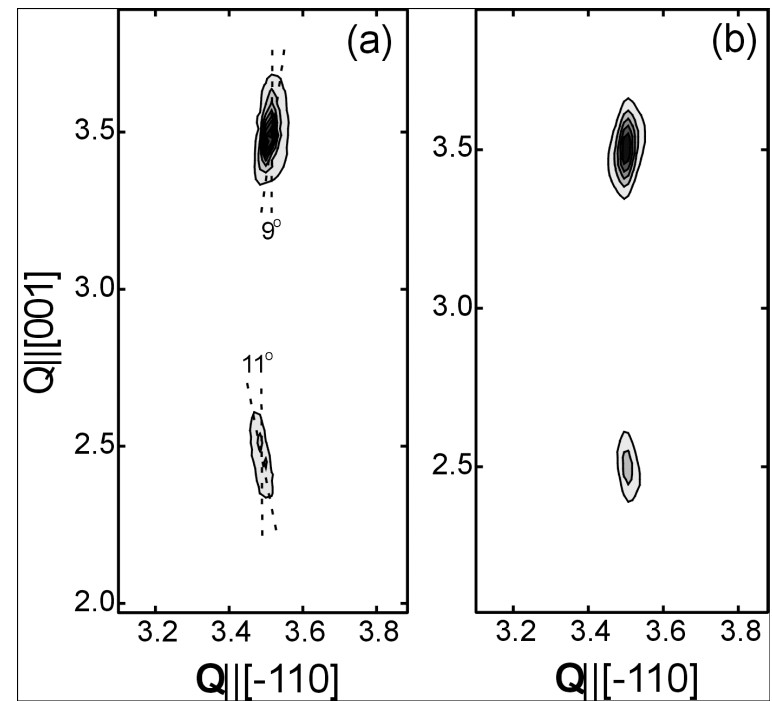
Single variant - Ga_{0.5}In_{0.5}P

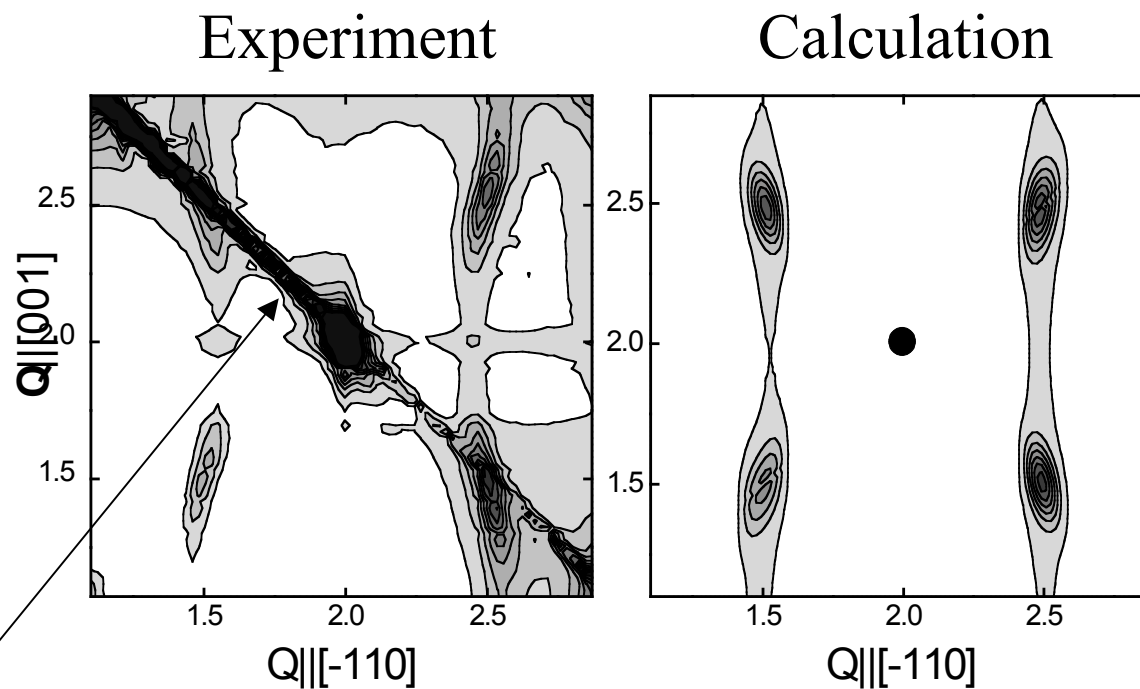


OAK RIDGE NATIONAL LABORATORY
U. S. DEPARTMENT OF ENERGY

UH

Double-variant Ga_{0.5}In_{0.5}P



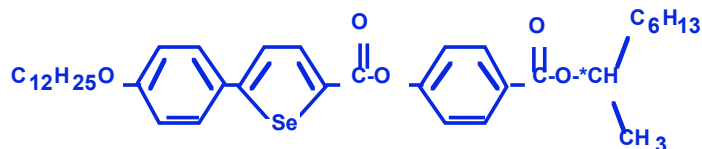
Double-variant $\text{Ga}_{0.5}\text{In}_{0.5}\text{P}$ 

This diagonal streak is from twinning and stacking faults that are not considered in simulation

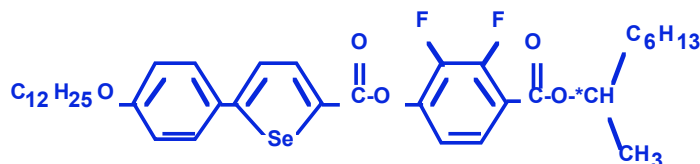


Antiferroelectric & ferroelectric liquid crystals- Helen Gleeson, U. of Manchester

New General User



K 67.7 SmC*_A 97.8 SmC*_{FI1} 99.0 SmC* 109.4 SmA 116.6 I
(Sml* 33.3 Sml*_A 42.2)



K 46.3 SmC*_A 82.6 SmC*_{FI1} 83.6 SmC*_{FI2} 86.3 SmC* 84.3 SmA 93.7 I

- Synthesised by Goodby (Hull/York University)
- Studied via optical and x-ray techniques
 - X14A to explore interlayer structure in smectic liquid crystals



OAK RIDGE NATIONAL LABORATORY
U. S. DEPARTMENT OF ENERGY

Resonant x-ray scattering

- Conventional x-ray scattering gives scalar information, e.g. size & position of layers, but cannot distinguish AFE, FI and FE. Sees (0 0 1), (0 0 2) peaks

$$Q_z = 2\pi l/d = l Q_0$$

- Scattering at an atomic absorption edge - resonant scattering gives tensor response
- Forbidden reflections occur reflecting interlayer periodicity, e.g. for AFE at (0 0 n+0.5)

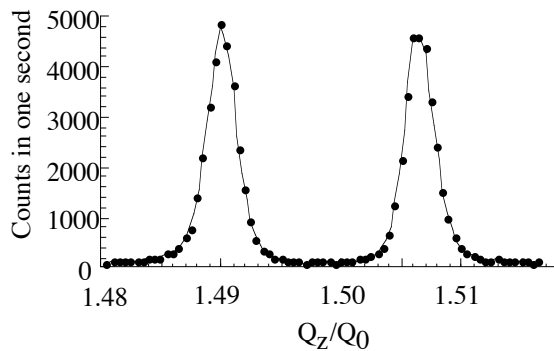
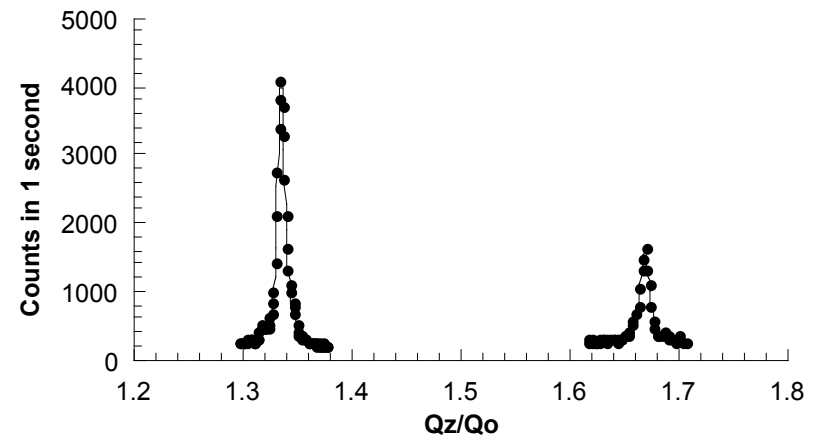
$$\frac{Q_z}{Q_0} = l + m \left(\frac{1}{n} + \frac{d}{p} \right)$$



Resonant signals

Resonant peaks occur at:

Phase	Q_z/Q_0
AFE	0.5, 1.5, ...
3-layer	0.33, 0.67, 1.33, ...
4-layer	0.25, 0.5, 0.75, ...



Polarization analysis -
clock model

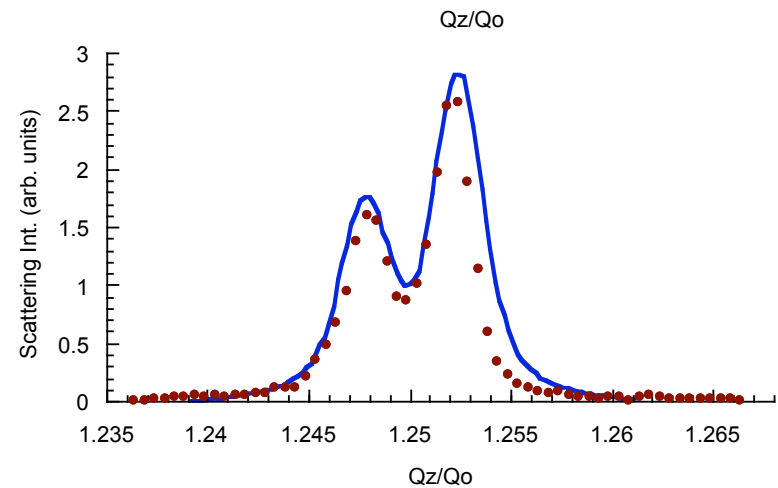
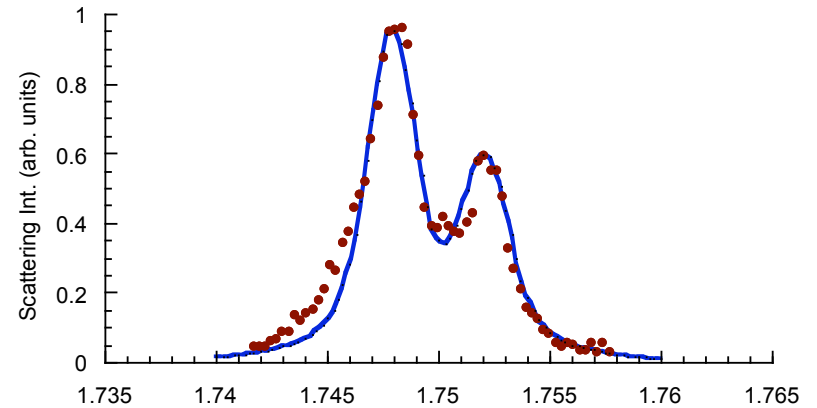
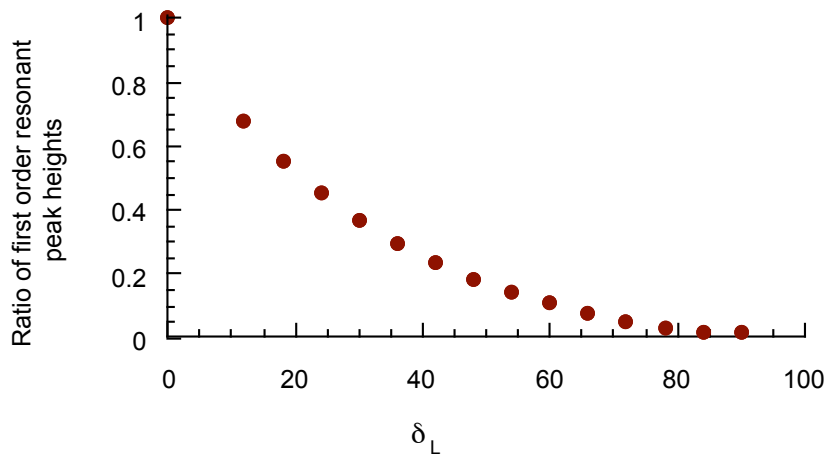
Peak splitting -
helical superstructure



Biaxial 4-layer phase

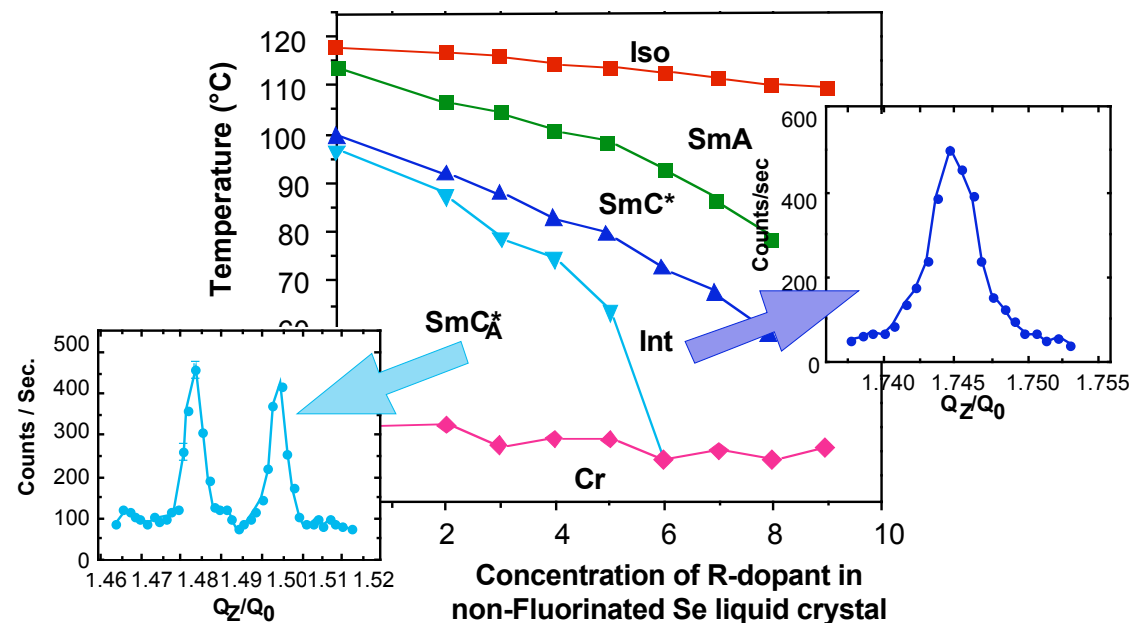
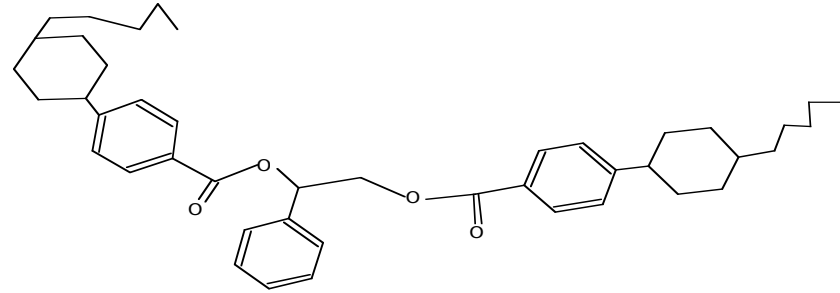
Distortion angle is $\sim 15^\circ$

Doesn't appear to be very temperature dependent



Is the 3-layer phase distorted too?

- Very 'fragile' phase
- Mixtures with chiral dopants increase intermediate phase range to $>15^\circ$
- Tilt decreases with concentration



Recent (Sept 04) measurements

- Very successful measurements on 3-layer phase
- Distortion angle is $\sim 40^\circ$

Pitch is ~ 181 layers
(550nm)

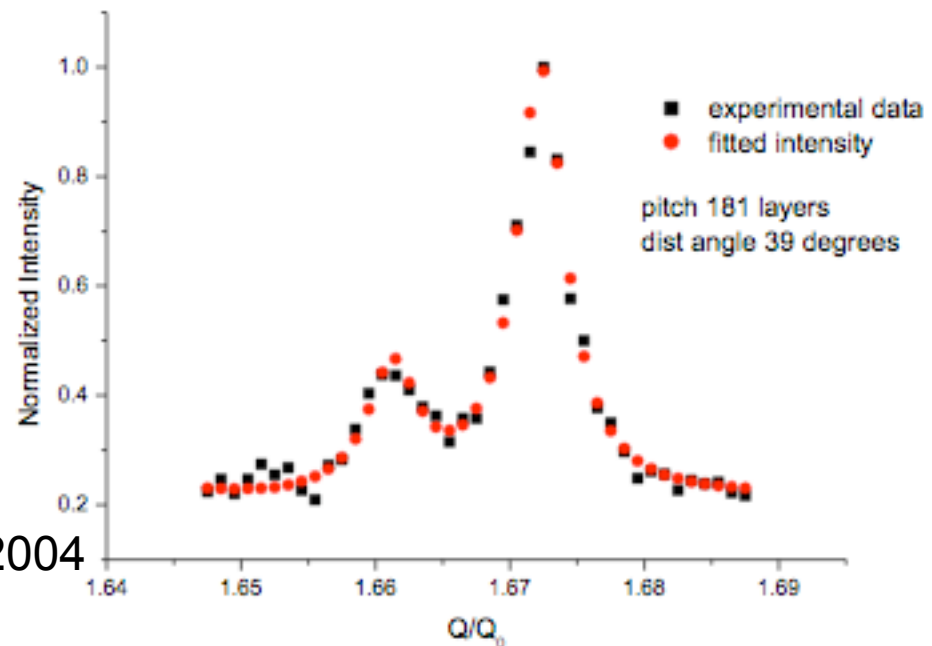
Temperature
dependence?

Invited Presentations:

- ✓ British Liquid Crystal Society, 4/2004
- ✓ Rank Prize Meeting, 12/2004
- ✓ 19th Thermo Conference, 5/2005

Publications:

- o (in progress)



Acknowledgement

The High Temperature Materials Laboratory User Program (primary PRT sponsor) is sponsored by the DOE Office of Freedom Car and Vehicle Technologies

(projects related to materials for vehicle technologies or other offices in DOE-EERE can apply for time via the HTML User Program, proposals reviewed monthly)

NSLS is sponsored by DOE - Basic Science



**OAK RIDGE NATIONAL LABORATORY
U.S. DEPARTMENT OF ENERGY**